AD-A094 622 COLD REGIONS RESEARCH AND ENGINEERING LAB HANOVER NH F/G 8/12
SINGLE AND DOUBLE REACTION BEAM LOAD CELLS FOR MEASURING ICE FO--ETC(U)
OCT 80 P R JOHNSON, J P ZARLING

UNCLASSIFIED CRREL-80-25 NL

1 OF 1
AD
A094622

END
DATE FILMED
3-81
DTIC

CRREL

LEVEL II

12

Single and double reaction beam load cells for measuring ice forces

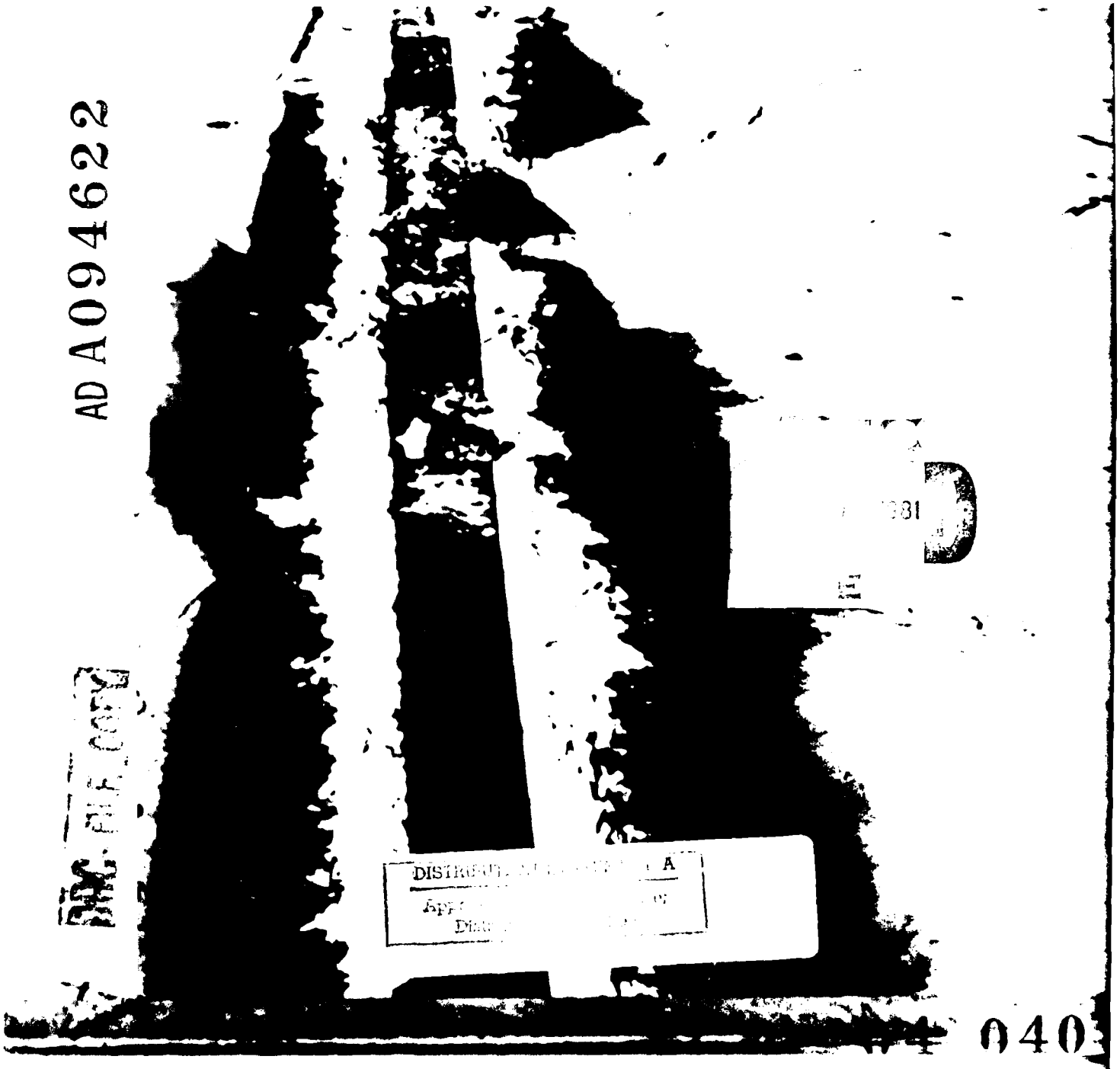

040

CRREL Report 80-25

Single and double reaction beam load cells for measuring ice forces

P.R. Johnson and J.P. Zarling

October 1980

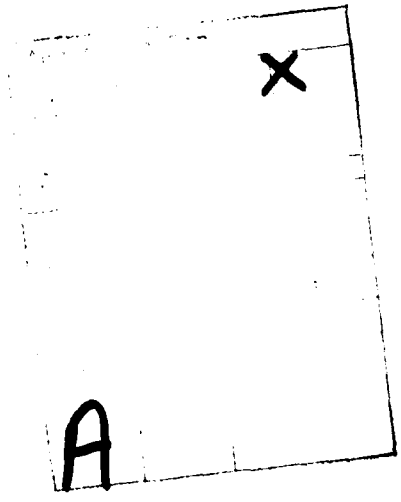

Prepared for
FEDERAL HIGHWAY ADMINISTRATION
By
UNITED STATES ARMY
CORPS OF ENGINEERS
COLD REGIONS RESEARCH AND ENGINEERING LABORATORY
HANOVER, NEW HAMPSHIRE, U.S.A.

Unclassified

SECURITY CLASSIFICATION OF THIS PAGE *(When Data Entered)*

REPORT DOCUMENTATION PAGE

READ INSTRUCTIONS BEFORE COMPLETING FORM

1. REPORT NUMBER: CRREL Report 80-25	2. GOVT ACCESSION NO.: AD A094122
3. RECIPIENT'S CATALOG NUMBER	
4. TITLE *(and Subtitle)*: SINGLE AND DOUBLE REACTION BEAM LOAD CELLS FOR MEASURING ICE FORCES	5. TYPE OF REPORT & PERIOD COVERED
	6. PERFORMING ORG. REPORT NUMBER
7. AUTHOR(s): P.R. Johnson and J.P. Zarling	8. CONTRACT OR GRANT NUMBER(s)
9. PERFORMING ORGANIZATION NAME AND ADDRESS: U.S. Army Cold Regions Research and Engineering Laboratory, Hanover, New Hampshire 03755	10. PROGRAM ELEMENT, PROJECT, TASK AREA & WORK UNIT NUMBERS
11. CONTROLLING OFFICE NAME AND ADDRESS: Federal Highway Administration, Washington, D.C. 20314	12. REPORT DATE: October 1980
	13. NUMBER OF PAGES: 20
14. MONITORING AGENCY NAME & ADDRESS *(if different from Controlling Office)*	15. SECURITY CLASS. *(of this report)*: Unclassified
	15a. DECLASSIFICATION/DOWNGRADING SCHEDULE

16. DISTRIBUTION STATEMENT *(of this Report)*

Approved for public release; distribution unlimited.

17. DISTRIBUTION STATEMENT *(of the abstract entered in Block 20, if different from Report)*

18. SUPPLEMENTARY NOTES

19. KEY WORDS *(Continue on reverse side if necessary and identify by block number)*

Ice forces
Ice loads
Instruments
Load cells
River ice

20. ABSTRACT *(Continue on reverse side if necessary and identify by block number)*

Two new types of load cells for attachment to bridge piers and direct measurement of ice forces were developed and tested with one type being installed on a pier of the Yukon River Bridge northwest of Fairbanks, Alaska. Both types of load cells used beams supported by base plates and carried nose plates that were loaded by the ice. The loads were imposed at the beams at locations differing from the support reactions so that the loads developed moments in the beams. By instrumenting them with strain gauges, the loads could be measured. Details of the design of the load cells, the means of calculating the loads and experience obtained with load cells are discussed.

DD FORM 1 JAN 73 1473 EDITION OF 1 NOV 65 IS OBSOLETE

Unclassified

SECURITY CLASSIFICATION OF THIS PAGE *(When Data Entered)*

PREFACE

This report was prepared by P.R. Johnson, Research Civil Engineer, and J.P. Zarling, Research Mechanical Engineer, of the Alaskan Projects Office, U.S. Army Cold Regions Research and Engineering Laboratory. The load cell development described in the report was funded during 1976-1978 by DA Project funds and, since mid-1978 under a research project, *Measurement and Prediction of Ice Loads on Bridges* sponsored by the Federal Highway Administration, U.S. Department of Transportation under their purchase order no. 8-3-0128. Dr. T.T. McFadden and J.R. Burdick assisted in the design, testing and installation of the various load cells. D. Dinwoodie, E. Culp, F. Fisk, M. Frank, R. Adams, K. Crane, C. Powell, J. Buska and R. Taylor assisted in the construction, instrumentation and installation of the cells. D.F. Garfield, F. D. Haynes and D. Cole carried out tests on the cells at CRREL in Hanover, New Hampshire. J. Burdick and F.D. Haynes technically reviewed this report.

Testing and laboratory equipment belonging to the University of Alaska and the Materials Laboratory, Alaska Department of Highways (now Alaska Department of Transportation and Public Facilities), was used in testing and calibrating various load cells.

CONVERSION FACTORS: U.S. CUSTOMARY TO METRIC (SI) UNITS OF MEASUREMENT

These conversion factors include all the significant digits given in the conversion tables in the ASTM *Metric Practice Guide* (E 380), which has been approved for use by the Department of Defense. Converted values should be rounded to have the same precision as the original (see E 380).

Multiply	*By*	*To obtain*
microinch	0.0254*	micrometer
inch	25.4*	millimeter
foot	0.3048*	meter
mile	1.609347	kilometer
pound-force	4.448222	newton
pound-force/inch^2	6.894757	kilopascal

*Exact

CONTENTS

ILLUSTRATIONS

Figure

TABLES

Table

SINGLE AND DOUBLE REACTION BEAM LOAD CELLS FOR MEASURING ICE FORCES

P.R. Johnson and J.P. Zarling

INTRODUCTION

The design of highway bridges and other river structures in the northern portion of the United States and in most of Canada and Alaska is controlled by the ice loads that may be imposed on the structure. Such forces may easily be an order of magnitude greater than those imposed by other environmental factors such as winds and currents. However, despite their importance, the magnitude of ice forces and the factors that control these forces are not well known. There are strong indications that design loads used in the past have been unduly conservative. Prior to 1974 both the Canadian and U.S. codes specified that an ice design pressure of 400 psi would be applied to the area that could be loaded by ice—the pier width multiplied by the anticipated thickness of ice. Field measurements of ice forces, particularly in Alberta, Canada, and recognition of the fact that bridges built to lower specifications did not fail indicated that code ice forces could be reduced. As a result, the Canadian bridge code was revised in 1974 to allow for reduced forces under many circumstances. The American Association of State Highway and Transportation Officials, the U.S. code group, adopted this 1974 Canadian bridge design code in 1978, and the Canadian Code was again altered in that year. The trend has been toward reducing ice design loads, which can lead to substantial reductions in bridge construction costs.

A bridge built across the Yukon River, about 90 air miles northwest of Fairbanks, Alaska (Fig. 1, 2 and 3), to support construction of the trans-Alaskan pipeline was opened to traffic in October 1975. It was immediately apparent that it would provide a very good site for obtaining field measurements of ice forces on the bridge piers since several piers in the river (see Fig. 4) would be subjected to a great deal of ice loading. A small group from CRREL's Alaskan Project Office, the University of Alaska and the Alaska Highway Department (now Department of Transportation and Public Facilities) became interested in a potential research project at the bridge and observed the 1976 breakup.

Some experimental load cells were constructed and considered for installation during the 1976 breakup but none were installed. An improved load cell using a single reaction beam (SRB) was designed and three were built and installed on the 90° tip of the nose of pier 5 of the bridge for the 1977 breakup. Figure 5 shows the nose of the pier, including the 1977 load cells. However, no data were obtained in 1977 due to recorder malfunction and subsequent failure of the load cells themselves under ice loading.

New SRB load cells were constructed and installed on the nose of pier 5 for the 1978 breakup, but abnormally low water flow resulted in a breakup where the ice mainly melted in place and an effective ice run did not occur. The three SRB load cells were replaced with stronger units for the 1979 breakup and two additional units were installed. An early breakup of strong ice occurred and some data were obtained. However, the ice tore four of the five units off the pier during the ice run. The data have not yet been evaluated.

Since the Yukon River Bridge piers have pointed noses (see Fig. 5), the load cells discussed above were designed to be attached to the tip of the nose and measure only horizontal axial loads imposed at that point. Instrumentation plans also called for the development and use of other load cells to measure horizontal ice loads on the two faces of the nose. These were christened "flat cells" since they would have a flat configuration to fit on the pier nose.

Work was initiated on flat cell design in 1977 but the first concept was unsatisfactory. The development of the SRB system suggested that two parallel reaction beams could be used for a flat cell. A model was built and tested; it exhibited the desirable features of the SRB system and the double reaction beam (DRB) design was adopted. Two units were being fabricated for installation on the Yukon River bridge for the 1979

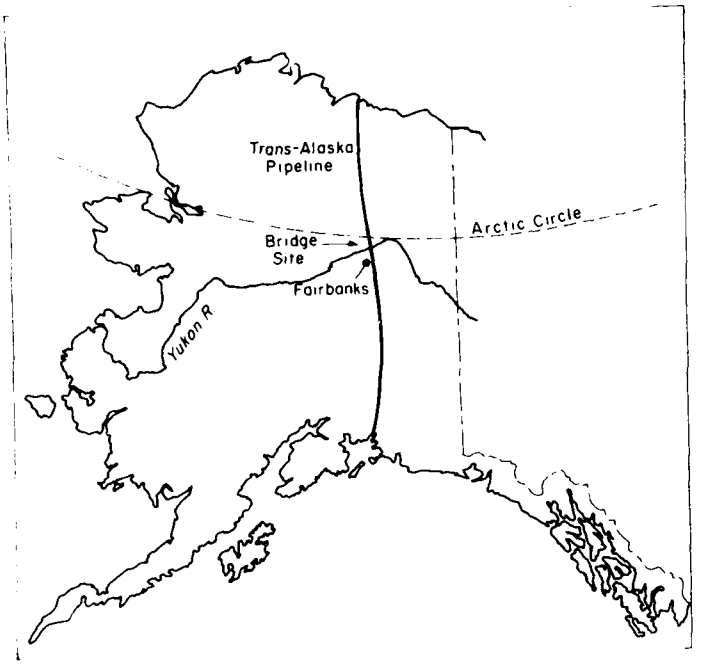

Figure 1. Location of the Yukon River Bridge.

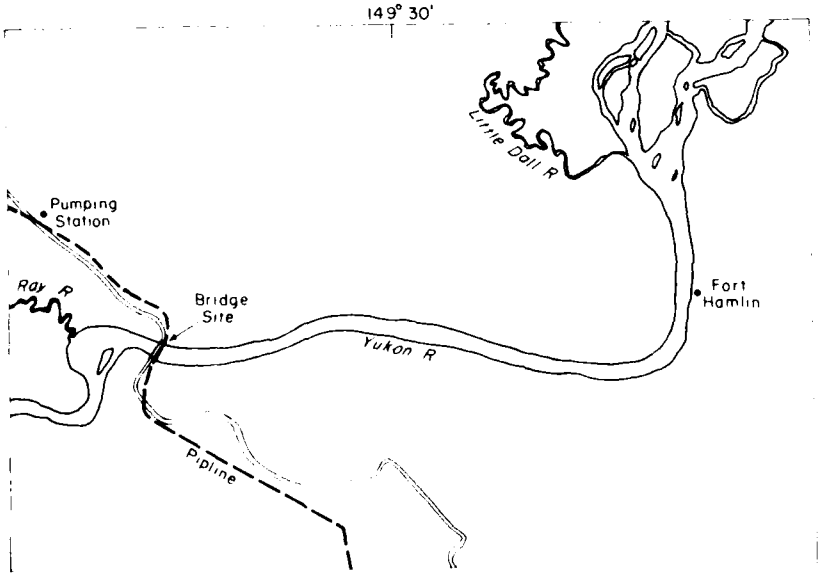

Figure 2. The immediate area of the Yukon River Bridge.

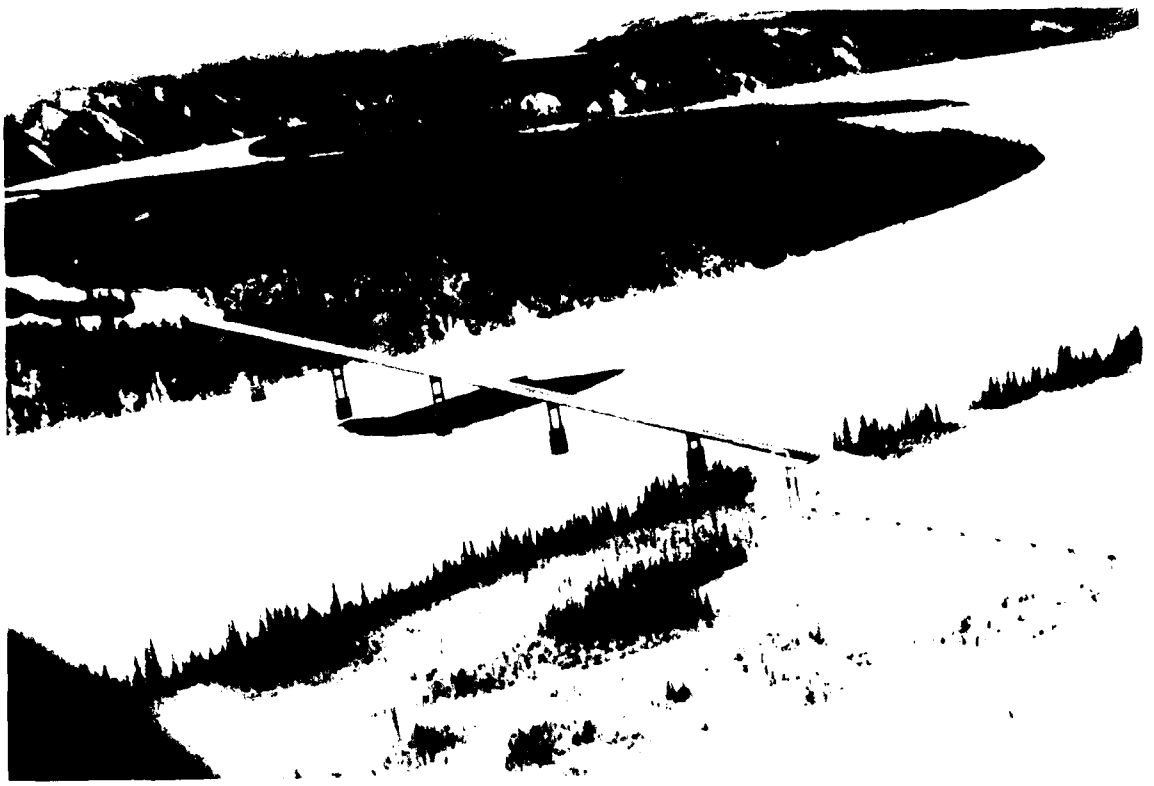

Figure 3. Aerial view of Yukon River Bridge.

Figure 4. Piers of the Yukon River Bridge.

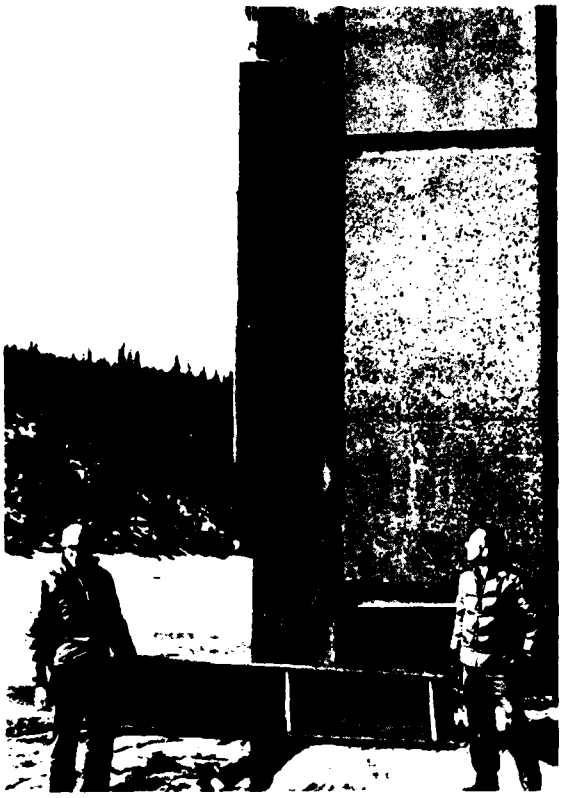

Figure 5. Pier 5 with three load cells in place.

breakup, but work on the units was stopped before they were completed and they were not tested on the bridge.

Work on both types of load cells was halted after the 1979 breakup due to reorientation of the project. This report has been prepared to describe the types of instruments developed and to summarize the information accumulated during their development, testing and operation.

ESTIMATES AND FIELD MEASUREMENTS OF ICE FORCES ON STRUCTURES

General

The techniques and equipment for making field measurements of ice forces on structures are not well-developed. Two general approaches have been used: indirect methods to estimate total forces and direct measurements of unit pressures or total forces on a structure. Various techniques that have been used are discussed below.

Indirect estimates

One of the earliest methods of indirectly estimating ice forces was Korzhavin's (1962) "kinematic" method which has been used in the U.S.S.R. Photogrammetry was used to estimate the mass and deceleration of an individual ice floe as it struck a bridge pier or other structure. From this information the estimated force of the ice on the pier could be developed. Michel (1970, Table VIII) reported the range of values obtained by Korzhavin which Neill (1976) thought were surprisingly small. This method has not been used in North America, although it was proposed to test it in the Yukon River Bridge ice study of which the load cell work described in this report is a part. It should be noted that this method can be used only in the case of an isolated floe of unknown area, thickness and velocity drifting downstream and striking an individual pier.

A number of studies have been made of the response of structures to ice loading. Sanden and Neill (1966) reported on the structural analysis of a number of old bridge piers that had withstood ice runs for up to 60 years in Alberta, Canada. Since they had not failed, ice forces that had been exerted over a very substantial length of time had obviously been less than those which would have caused failure. Danys (1972) reported on structural analyses of 22 offshore light piers in the St. Lawrence Waterway of which 7 had been damaged or destroyed by ice. This report separated cases of failure from those of survival. Reinius et al. (1971) and Bergdahl (1972) reported analyses of two lighthouses in the Baltic Sea which failed under ice loads. Efforts have been made to measure acceleration forces on a bridge under ice loading in Alberta, Canada. Similar efforts were made to measure acceleration forces on piers of the Yukon River Bridge during the 1978 and 1979 breakups. Data obtained during the 1979 breakup have not yet been analyzed.

The studies of structures which have either resisted, or failed under, ice loading provides extremely useful information by establishing limits to ice forces. Normally lacking, however, is such information as ice structure, thickness and strength, rafting, temperatures, thermal history, etc. Also lacking is information on the effects of dynamic ice loading such as that reported by Engelbrektson (1977) where the dynamic response and resonance of a lighthouse led to a greatly increased total force. Perhaps a final limitation of this approach is that there are only a few structures that will give information of value.

Direct measurements

Direct measurements of ice forces and pressures may be considered to begin with Gamayunov (Korzhavin 1971) who suspended a hinged plate in front of a pier

of a bridge across the Dniepr River at Kiev, U.S.S.R. The plate was supported by hydraulic dynamometers. Data were collected but the equipment was deficient and the information obtained has not been considered trustworthy.

Peyton (1966) was the first to obtain reliable field measurements of ice forces using a hinged beam. A hinged beam consists of a relatively rigid and strong vertical or inclined beam extending from a hinge below the water line through the ice to a support at the top of the beam. The support is instrumented to measure loads at that point. The elevation of the ice impact can be determined visually, photographically or by using a water level recorder and, with the ice impact level known, the ice load can be calculated. Peyton's measurements were made in the floating ice sheets of Cook Inlet, Alaska.

The Alberta Cooperative Research Program installed hinged beams on two bridges in Alberta, Canada, with the first data obtained in 1967 and 1969 for the two sites. Figure 6 shows the Hondo installation on the Athabasca River. A summary of the data through 1974 is found in Neill (1976). It is considered that these installations have produced the best measurements of ice loads on bridge piers, but it should be noted that 1) the data are for one small and one medium-sized river in central Alberta, and 2) a hinged beam has certain inherent limitations.

Blenkarn (1970) measured ice forces in Cook Inlet using a test pile driven into the sea bed, a four-legged permanent platform and other structures. On the four-legged platform, data were obtained from strain gauges installed on cross-members and a computer analysis of the structure.

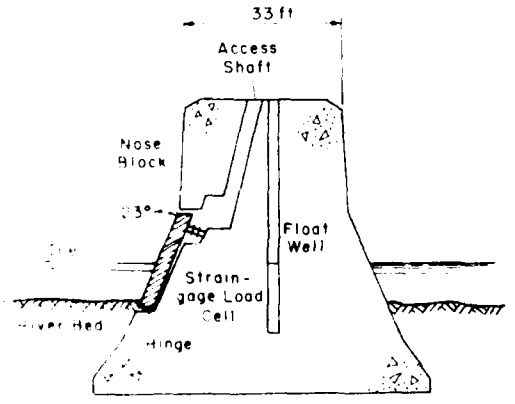

Figure 6. Section of Hondo Bridge, Alberta, Canada, showing hinged beam load cell (after Neill 1976).

Schwarz (1970) installed 50 small pressure-measuring plates on a vertical pile in the Eider River, West Germany. In this coastal Baltic location, sea ice forms just outside the estuary of the river and is carried upstream by tidal currents. Each plate covered a small portion of the pile and measured ice forces in its discrete area.

Danys (1975) reported on the instrumentation of a conical light pier in the St. Lawrence Waterway. A number of panels, each supported by four load cells in the corners, were installed in the ice zone. Remote operating and data transmission systems were installed.

Croasdale (1974) carried out a number of "nut-cracker" tests in the ice of the Mackenzie River Delta, Canada. Two steel pipes, hinged at the bottom, were frozen into the ice. When the desired thickness of ice had formed, the two pipes were jacked apart while the applied force was measured.

Garfield and Zabilansky* instrumented a pile anchored into the bed of the St. Clair River to measure ice forces. Data were obtained during the 1977–78 spring breakup. A second structure was scheduled to be installed in the St. Clair River in late 1979 near the shipping channel to measure dynamic ice forces.

Garfield, Nevel and Zabilansky* designed and constructed a "total load" device to be mounted on a bridge crossing the Ottauquechee River, Vermont. The device, however, was not completed in time to be installed for the 1979 breakup.

J. Burdick† designed and constructed a "total load" device to be used on the Yukon River Bridge. This device was also completed too late to be installed for the 1979 breakup.

With the exception of the data obtained in Alberta, Canada, no full-scale data are available on the loads exerted by freshwater ice on bridge piers. Most of the data (Peyton 1977, Blenkarn 1970, Schwarz 1970 and Croasdale 1974) were for sea ice, and Danys' information was obtained for conical structures. The data obtained by Garfield and Zabilansky have not yet been fully analyzed and published.

Two types of devices have provided useful and reliable data of the sort that is of interest to this study. The hinged beam used by Peyton (1966) and by the Alberta Cooperative Research Program has worked extremely well and has perhaps provided the basic data against which results obtained from other devices should be examined. The small load cells installed by Schwarz (1970) also provided very good data.

*D. Garfield, D. Nevel and L. Zabilansky, CRREL, personal communication, 1979.

†J. Burdick, Civil Engineering Department, University of Alaska, personal communication, 1979.

Small-scale and laboratory studies

In addition to the indirect and direct methods that have been used to estimate or measure ice loads, numerous small-scale and laboratory studies have been made. This work, together with various theoretical studies, has suggested or identified many factors which may need to be considered in predicting ice forces against a structure. These include ice strength, the area of ice contact, the shape and inclination of the pier nose, ice velocity, aspect ratio (pier width:ice thickness), the contact coefficient and a number of other factors.

INSTRUMENTATION PLAN FOR MEASURING ICE LOADS ON THE YUKON RIVER BRIDGE

The investigators decided to use two approaches to measure ice forces on the Yukon River Bridge: use of a "total load" device to be designed by J. Burdick that would ride on the pier nose and use of smaller load cells designed by the authors to be directly attached to the bridge. Zarling carried out the single reaction beam (SRB) studies and Johnson the double reaction beam (DRB) studies. This report discusses the SRB and DRB studies but not development of the "total load" system which is still continuing.

It is recognized that the shape of the nose of a pier will affect the force that ice can exert on the pier, and a variety of shapes have been used. The pier nose may be vertical or inclined. The cross section can be blunt (rectangular), semicircular or pointed (wedge-shaped). Different combinations can be used. For example, the Hondo bridge in Alberta (Fig. 6) has a semicircular inclined nose while its companion instrumented Alberta bridge has a semicircular vertical nose. Tryde (1977) conducted tests on a model pier with an inclined pointed nose.

The inclined pier nose tends to reduce total forces because it can change the failure mode of the ice from crushing to bending (Neill 1976). Since ice is weak in tension and bending failure is tensile, ice loads may be reduced. The pointed pier nose tends to cause splitting of the ice sheet impinging on the pier and may also reduce ice forces. The piers of the Yukon River Bridge have pointed vertical noses (Fig. 4 and 5). These concrete piers are about 70 ft high, 9 ft wide and 40.5 ft long, including the pointed ends.

Several modes of ice failure were observed at the Yukon River Bridge but the principal modes were crushing or crushing and splitting. A typical idealized sequence is shown in Figure 7. A large ice sheet or floe striking a pier would initially fail by crushing as it engages the nose of the pier as in Figure 7b. As the floe continues onward, the crushing front widens until it extends across the entire nose of the pier as in Figure 7c and then continues farther until the pier is partially or completely enveloped within the floe as in Figure 7d. At this point the floe may continue to crush, or the tensile forces that are generated in the ice may cause splitting as shown in Figure 7e. This will relieve loads on the tip of the nose. However, as the ice sheet continues to move, the crack will deviate from the tip of the pier nose and will progress farther and farther to one side of the pier until the tip of the nose is detaching blocks from the ice as in Figure 7f. With further motion the crack will miss the nose of the pier and crushing will again be established across the pier nose. This may initiate a new cracking cycle.

In the above sequence, the tip of the pier nose may be loaded with a balanced axial load due to crushing and then the load may be partly or entirely relieved by splitting. The maximum loads are probably experienced during crushing on the full nose of the pier. On the basis of this model, the SRB load cell for the tip of the nose was designed to measure only axial loads but yet had to be strong enough to resist unbalanced lateral loads.

The situation is different farther along the nose of the pier as at point A, Figure 7c. The sides of the vertical, pointed pier nose are loaded by two ice forces, the normal force F_n and the frictional force F_f of ice sliding along the pier as shown in Figure 8a. However, the coefficient of friction of warm, wet ice on a smooth, warm and wet structure is small; Kuroiwa (1977) found the coefficient of kinetic friction of a skate runner on warm (but not thawing) ice to be on the order of 0.005. Other reports indicate that it may be as high as 0.05. In either case the friction forces are very small compared to the normal forces and can be ignored for the present. A load cell at point A in Figure 8c need only measure normal forces.

The normal force F_n can be separated into two components, the horizontal axial force F_a and the horizontal transverse force F_t as shown in Figure 8b. These can be calculated as

$$F_a = F_n \sin\alpha \qquad (1)$$

$$F_t = F_n \cos\alpha \qquad (2)$$

where α is the half-angle of the nose as shown in Figure 8. F_a is the force resisting the axial movement of the ice while F_t is the lateral force which generates a tensile stress in the ice.

At this point one can see why splitting occurs only after the ice has partly or fully enveloped the pier (Fig. 7d), rather than when it first fully contacts it (Fig. 7c). If ice were to break due to lateral loads (Fig. 7c), small blocks, such as indicated by the dashed line, would break out of the ice. This, however, is probably unimportant compared to the crushing and cracking sequence shown in Figures 7d and 7e where large ten-

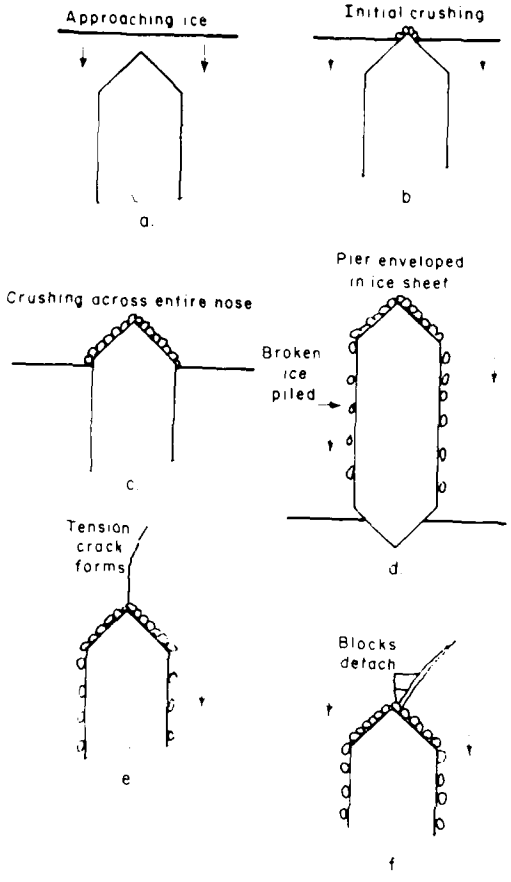

Figure 7. Crushing and splitting sequence.

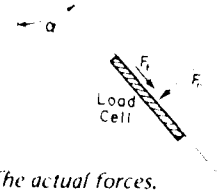

a. The actual forces.

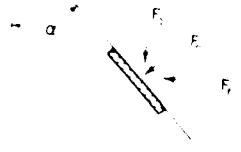

b. The important component forces.

Figure 8. Ice forces on a load cell installed on the face of a pointed pier.

sile stresses build up in the ice and cracks can be propagated ahead of the pier.

Other forces might also be considered. One is the gravity force resulting from the need to move the broken ice onto the top of the ice sheet and into the water under the ice sheet. While this is important in the case of an icebreaker, it is believed to be very small when ice is crushing against a relatively narrow bridge pier and will be ignored. A second force to consider is the frictional drag of the ice against the sides of the pier. Again, this force is important in the case of an icebreaker, but it is believed to be very small in the case under consideration and will be ignored.

Based on the above analysis, it seemed necessary only to install load cells on the tip of the pier to measure horizontal axial forces and additional load cells farther along the flat sides of the pier nose to measure normal forces. This is the system that was followed and is described below.

LOAD CELL DEVELOPMENT

The load cells designed and installed in 1979 to measure nose-tip axial forces for the 1979 Yukon River breakup evolved from designs developed for the 1976, 1977 and 1978 breakups. During the winter of 1976–77 a load cell was designed based on an instrumented simply-supported beam (now called a reaction beam) within each load cell. As shown in Figure 9, the load on the nose was imposed on the reaction beam at two points offset from the two supports rising from the base so that a load on the nose would generate moments in the beam. Strain gauges were installed: those in 1977 between each load and its nearby reaction and those for 1978 and in later designs inside the loading system. The load vs strain gauge output of this design was quite linear and reproducible.

Three load cells using this design were built and installed on the nose of the pier for the 1977 breakup. Figure 10 shows an exploded view of a load cell and Figure 5 shows the three units attached to the pier.

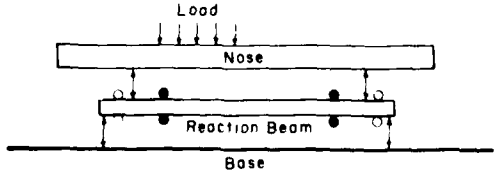

Figure 9. Schematic diagram of a single reaction beam system. o indicates strain gauge location on the 1977 units. • indicates strain gauge location on later units.

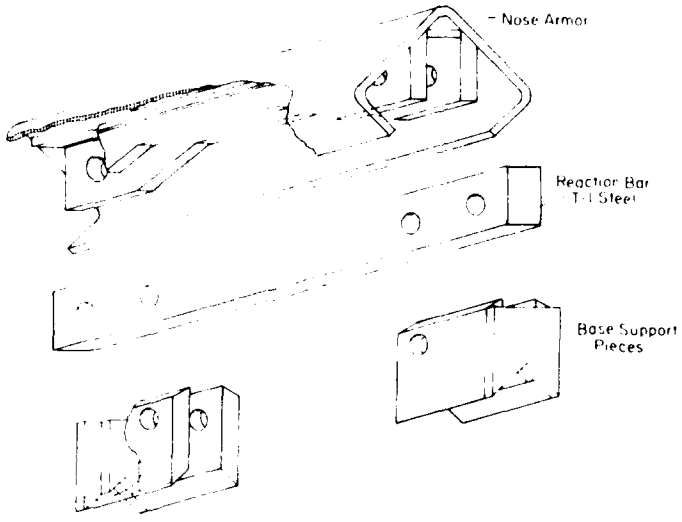

Figure 10. Exploded and cut-away view of SRB load cell.

The installation was completed only a few hours before the ice went out, not allowing sufficient time to check out the electrical/recording system. Ink freezing in the recorder pens and faulty amplifiers in the recorder precluded acquisition of data during the intial hours of breakup. Before all of the electrical problems were debugged, the load cells failed due to ice forces.

Stronger units were built and installed on the bridge for the 1978 breakup but low water levels and ice jamming at the bridge prevented acquiring any data. The three load cells installed for the 1978 breakup were strengthened and two additional units were built and installed for the 1979 breakup. Data, which had not been analyzed at the time of writing, were obtained during the 1979 breakup, but again the ice forces ultimately tore the units from the pier. All of these units presented a pointed face to the ice to reproduce the shape of the pier nosed tip.

The instrumentation plan also called for flat cells to be installed on the nose of the pier on both sides of the SRB units. This would have protected the SRB units from much of the lateral ice forces and probably prevented their loss, particularly during the 1979 breakup.

THE SINGLE REACTION BEAM SYSTEM

The schematic drawing of the single reaction beam (SRB) load cell (Fig. 9), shows that it consists of a nose piece, an instrumented reaction beam and a base. The nose piece receives the applied load and transmits it to the reaction beam. Since the nose forces and the base support forces are applied at different locations on the reaction beam, bending moments are developed in the beam. The strains caused by these moments can be measured with strain gauges. From this information the total load or the magnitude and location of an equivalent point load can be determined.

All connections are pin connections. The generalized geometry of the reaction beam system is shown in Figure 11. Various subscripts indicate the quantity being measured. L_n indicates the length of the nose, L_r is the length between reactions, etc. The distance between two points at one end of the unit is indicated by a double subscript such as L_{nr}, for example, which can be calculated as $L_{nr} = (L_n - L_r)/2$.

To analyze the bending moments and strains developed in the reaction beam due to a generalized loading, assume that an equivalent point load P is applied on the nose some distance X from the left end of the nose piece as shown in Figure 11. The reaction beam supports the nose at D_1 and D_2 and is supported by two reaction forces, R_1 and R_2. The two loads, D_1 and D_2 can be determined by summing moments around D_2 and D_1 respectively as shown in Figure 12:

$$D_1 = P\frac{L_d + L_{nd} - X}{L_d} \tag{3}$$

$$D_2 = P\frac{X - L_{nd}}{L_d} \tag{4}$$

and, by summing forces,

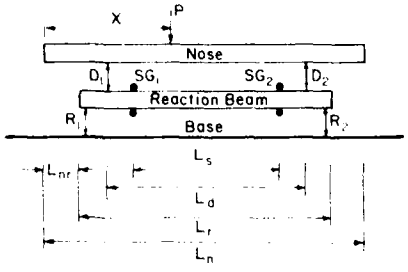

Figure 11. Generalized dimensions of the single reaction beam system (lengths are in inches).

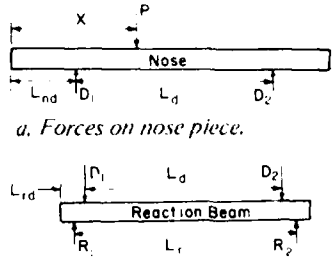

a. Forces on nose piece.

b. Forces on reaction beam.

Figure 12. Forces on the nose piece and reaction beam.

$$D_1+D_2 = P. \tag{5}$$

The reactions R_1 and R_2 can be determined by summing moments at R_2 and R_1 in Figure 12b:

$$R_1 = \frac{D_2 L_{rd}+D_1(L_{rd}+L_d)}{L_r} \tag{6}$$

and

$$R_2 = \frac{D_1 L_{rd}+D_2(L_{rd}+L_d)}{L_r}. \tag{7}$$

Upon substituting eq 3 and 4 into eq 6 and 7, R_1 and R_2 can be expressed in terms of load and primary reaction beam geometry:

$$R_1 = P\frac{L_r+L_{nr}-X}{L_r} \tag{8}$$

$$R_2 = P\frac{X-L_{nr}}{L_r}. \tag{9}$$

Summing eq 8 and 9

$$R_1+R_2 = P. \tag{10}$$

Shear and moment diagrams for the reaction beam are shown in Figure 13. Values of shear are equal to the reactions at the respective ends of the reaction beam and to R_1-D_1 between D_1 and D_2. The maximum shear is equal to the maximum reaction. At each end of the beam the moments increase from zero to a value of RL_{rd} and the larger of R_1 and R_2.

Because M_1 and M_2, the moments at SG_1 and SG_2, are symmetrically positioned on the beam and the moment distribution is linear between D_1 and D_2, the sum of M_1 and M_2 is equal to the sum of the moments at locations D_1 and D_2. Therefore

$$(R_1+R_2)L_{rd} = M_1+M_2. \tag{11}$$

Substituting eq 10 into eq 11 and solving for P yields

$$P = \frac{M_1+M_2}{L_{rd}}. \tag{12}$$

M_1 and M_2 can be determined by taking moments about the points SG_1 and SG_2:

$$M_1 = R_1 L_{rs}-D_1 L_{ds} \tag{13}$$

and

$$M_2 = R_2 L_{rs}-D_2 L_{ds}. \tag{14}$$

Substituting eq 3, 4, 8 and 9 for D_1, D_2, R_1 and R_2 into equations 12 and 13 and then subtracting and rearranging yields

$$M_1-M_2 = \frac{PL_{rs}}{L_r}(L_n-2X)-\frac{PL_{ds}}{L_d}(L_n-2X). \tag{15}$$

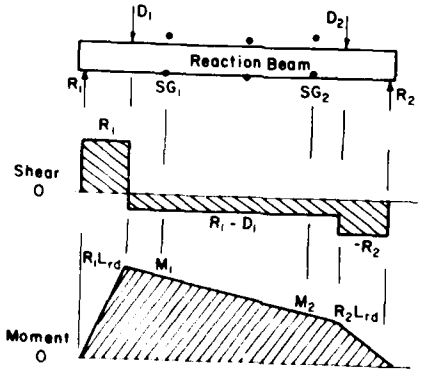

Figure 13. Reaction beam shear and moment diagrams.

Substituting the value of P in eq 12 into eq 15 and solving for X gives

$$X = \frac{L_n M_2}{M_1 + M_2}. \tag{16}$$

The load can also be determined from moments measured at the center of the reaction beam. It was shown in eq 12 that

$$P = \frac{M_1 + M_2}{L_{rd}}.$$

However, Figure 13 shows that the moment at the center of the beam is equal to the average of M_1 and M_2, or

$$M_c = \frac{M_1 + M_2}{2}. \tag{17}$$

Upon combining eq 10 and 17

$$P = 2M_c/L_{rd}. \tag{18}$$

Thus, by measuring strain at the center of the beam, the total load P on the load cell can be found. (J. Tiedemann, Department of Mechanical Engineering, University of Alaska, first brought this to our attention. The location of the equivalent point load cannot be determined if only M_c is used.)

For an elastic beam undergoing small deflections, the bending moments are proportional to the strain at any beam section, as given by the relationship

$$M = C\epsilon \tag{19}$$

where C is a proportionality constant (for a beam with a rectangular cross section, $C = Ebd^2/6$) and ϵ is strain. The beam is normally instrumented with strain gauges as shown in Figure 13. The moments at these sections can then be determined by using the known characteristics of the strain gauges and the beam. Both P and X can be found by using eq 12 and 16. Calculations illustrating the use of a SRB device are given in Appendix A.

PERFORMANCE OF A SINGLE REACTION BEAM LOAD CELL

A small SRB load cell was built, instrumented and tested in Alaska during late 1978 and then further tested under dynamic loading conditions and in an ice pit at Hanover, New Hampshire, in early 1979. The objectives of the tests were to 1) determine the sensitivity, linearity and reproducibility of the device under static loading conditions, 2) test the device under dynamic conditions, and 3) determine its performance in ice. The tested load cell had an 18-in.-long nose constructed from 4× 4× ¼-in. square structural tubing with one corner removed to allow it to be mounted on a reaction beam and with the opposite corner providing a 90° nose. All connections were pinned. The reaction beam was of 1× 2× 15-in. TI steel. Dimensions of the bar were as follows: L_r = 13 in., L_d = 9 in., and L_n = 6 in. Pairs of weldable 120-ohm Micro Measurements strain gauges were installed on the reaction beam, one of each pair on the top of the bar to measure compressive strain and the other on the bottom to measure tensile strain. The model was installed in a loading machine at the University of Alaska in Fairbanks and loads were increased in increments of 2500 lbf to a total of 15,000 lbf. The loads were also removed in the same increments. The data obtained are shown in Table 1.

Table 1. Loads and strain readings, static test.

Load (1000 lbf)	*Strain, top of cell (μin./in.)*	*Strain, bottom of cell (μin./in.)*	*Sum of strain (μin./in.)*
0	0	0	0
2.5	265	230	495
5.0	520	470	990
7.5	770	700	1470
10.0	1015	930	1945
12.5	1250	1150	2400
15.0	1490	1375	2865
12.5	1290	1155	2445
10.0	1045	920	1965
7.5	800	690	1490
5.0	545	460	1005
2.5	275	200	495
0	15	0	15

It was shown (in eq 12) that the sum of the moments (and thus the sum of the strains) are proportional to the total load. The strains measured at each load were added and the sum of the strains plotted against load in Figure 14. Table 1 and Figure 14 show the various values obtained. A linear regression of the data gives the equation

$$P = -115 + 10.4(\epsilon_1 + \epsilon_2)$$

with a correlation coefficient of 0.99.

It was concluded as a result of this and other tests that the SRB load cell was strong, sensitive, linear and produced reproducible results under axial static loading.

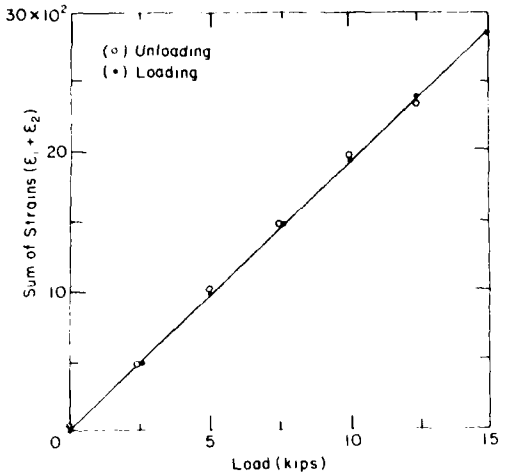

Figure 14. Half-scale SRB load cell test of sum of strain vs applied load.

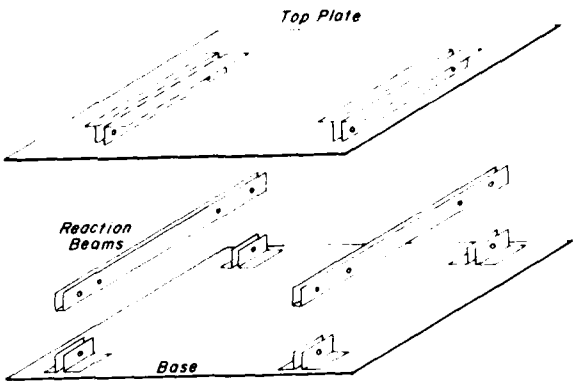

Figure 15. Sketch of a double reaction beam device.

Dynamic testing and testing in ice was carried out at CRREL in Hanover, New Hampshire (Cole 1979). Dynamic tests were run on an MTS machine with a mean load of 6500 lbf and a superimposed sinusoidal load of 6000 lbf, giving a minimum load of 500 lbf and a maximum load of 12,500 lbf. Later the loads were reduced to a load cycling between 500 and 4500 lbf to avoid deforming the nose of the cell. Loading frequencies were 1, 4, 8 and 16 Hz. It is estimated that more than 20,000 cycles were applied. Performance of the device was satisfactory.

The load cell was then tested in an ice pit with about 7 in. of ice, although calculations had shown the unit would probably sustain only about 5 in. of ice. A hydraulic ram was used to drive the unit 12 in. through the ice in 20 s at a constant speed. The loading system was not completely rigid so the load cell wandered somewhat. The maximum load applied was probably in excess of 25,000 lbf. Since this exceeded the design strength of the load cell, the nose piece deformed.

As a result of these tests, it was concluded that a SRB load cell would perform satisfactorily under dynamic conditions and in ice if properly designed and installed.

THE DOUBLE REACTION BEAM LOAD CELL

The SRB load cell is valuable for measuring axial loads on a narrow linear area. When loads must be measured on a larger area it is possible to use a pair of reaction beams to form a square or rectangular load cell. Figure 15 shows a schematic diagram of such a device. It consists of a cover plate, two parallel reaction beams and a base plate. Loads applied to the cover create moments in the reaction beams which can be determined from strain gauge measurements.

This device has several useful characteristics. The load cell can be made in a variety of shapes. It can also be instrumented, as will be described later, in a number of ways with the amount of information obtained increasing as the complexity of the instrumentation is increased. It shares with the SRB unit the characteristics of strength, sensitivity, linearity and simplicity.

Two units were designed and partially built for the 1979 breakup but they were not completed nor used in the field. Figure 16 shows a view of one unit, and its design theory is developed in more detail in Appendix B. These devices have been studied to some extent in the laboratory but minor problems that may trouble them under field conditions have not been identified.

REACTION BEAM DESIGN

Stress in the beam

The flexure formula for a uniform rectangular beam undergoing elastic deformation is

$$M = \frac{\sigma_b I}{c} \tag{20}$$

where M is the moment at a section in the beam (in.-lb), σ_b is the flexural stress (psi), I is the moment of inertia (in.^{4}) and c is the distance from the neutral axis to the surface of the beam (in.).

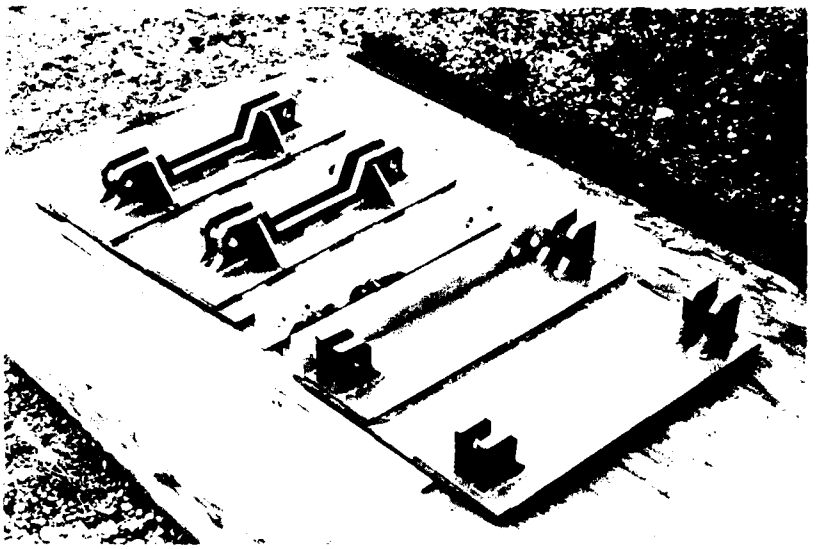

Figure 16. Photo of double reaction beam device.

The moment of inertia for a rectangular beam is $bd^3/12$ where b is beam width, d is beam height, both in inches, and c is $d/2$. Equation 20 can be rewritten as

$$\frac{6R\,L_{rd}}{\sigma_b} = bd^2 \qquad (21)$$

where $R\,L_{rd}$ has been substituted for M.

The maximum reaction R and the design strength σ_b of the material to be used will normally be selected by the designer. With these values substituted into eq 21, the designer can select a value of L_{rd} and then try various values of b and d until the best combination is found.

Deflection

The maximum deflection of the fully loaded reaction beam must be found to determine the clearance required between the beam and the base. The maximum deflection Δmax of a fully loaded symmetrical beam is given by the equation

$$\Delta\text{max} = \frac{PL_{rd}}{48EI}\left(3L_{rd}^2 - 4L_{rd}^2\right) \text{in.}$$

where E is the modulus of elasticity of the beam (psi). The maximum deflection with symmetrical loading is at the center of the beam.

Axial tensile stress in the reaction beam

The possibility that the deflection of a reaction beam will generate a tensile stress in the beam which, in turn, will lead to erroneous strain readings and calculated loads was examined. Any bending of the beam will shorten the distance between the ends. If the ends are firmly held, an axial tensile stress will develop in the beam. The associated strain will affect all strain gauges on the beam uniformly. The questions are 1) will axial strains be developed, and 2) what effect will the added strain have on the loads that are calculated?

Calculations showed that the shortening will be very slight for relatively stiff reaction beams such as those being used in the load cells discussed in this report. The shortening is estimated to be less than the play in the pin connections so that the prospects are that axial tensile stress will not develop. When both tensile and compressive strains are read in pairs in a half-bridge or two pairs are read in a full bridge, the uniform axial strain cancels out and has no effect on the bridge readings. Thus, the axial tensile stresses probably will not develop and, if they do, they will not affect the readings obtained or the loads that are calculated.

MEASUREMENT TECHNIQUES

The basic measurement technique for an SRB instrument is to install two pairs of strain gauges on each reaction beam, one at each end as shown in Figure 9. Each pair consists of a gauge on top to measure compressive strain and the other on the bottom of the beam to measure tensile strain. Each pair is read as a half-bridge as shown in Figure 17a. Under static conditions, the reading device can be switched from one pair of gauges to the other, but under dynamic conditions, two reading devices are required. Both the total load and the location of the equivalent point load can be found from the data as pointed out earlier.

If only the total load is required, the four strain gauges can be wired into a full bridge as in Figure 17b. Alternatively, the four gauges can be replaced with a pair at the center of the beam which can be read as a half-bridge.

The instrumentation of a DRB unit is similar to that of the SRB device. Each reaction beam is instrumented with strain gauges as shown in Figure 18. Each pair of gauges can be read in a half-bridge configuration. The magnitude and location of the equivalent point load on each beam can then be determined and the magnitude and location of the equivalent point load on the entire load cell can be found (see App. B). Alternatively, the eight strain gauges can be wired into a single series full bridge, as shown in Figure 17c, to determine the total load on the load cell with a single reading. Again, if only the total load is required, the four strain gauges on each reaction beam can be replaced with a pair at the middle of the beam and the four gauges read as a single full bridge.

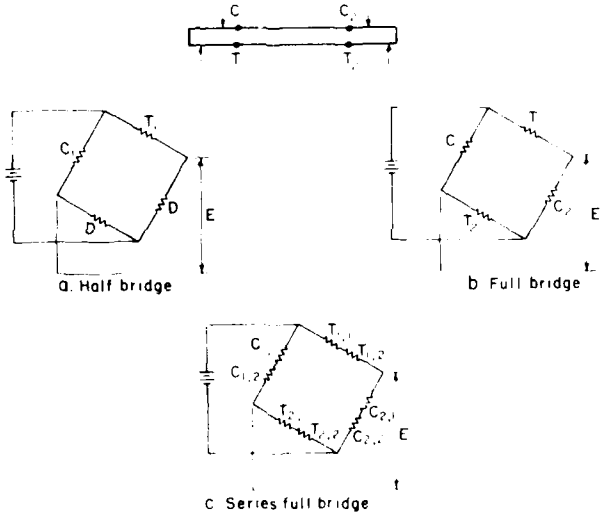

Figure 17. Wiring techniques for a SRB unit (a and b) and a DRB unit (c).

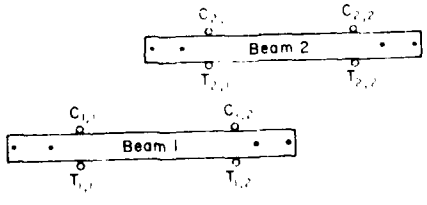

Figure 18. Strain gauges on a DRB unit.

CONCLUSIONS

The reaction beam load cells instrumented with strain gauges appear to be useful and versatile devices for measuring loads and forces. As a single reaction beam, it is the basis of the SRB load cells which were installed on the Yukon River Bridge to measure ice forces. As a double reaction beam device, it offers promise as a "flat cell" type of load cell. Both devices are linear, strong, sensitive and give reproducible results.

LITERATURE CITED

Bergdahl, L. (1972) Two lighthouses damaged by ice. *Proceedings of 2nd International Symposium, International Association of Hydraulic Research, Leningrad.*

Blenkarn, K. (1970) Measurement and analysis of ice forces on Cook Inlet structures. *Proceedings, Offshore Technology Conference.*

Cole, D. (1979) Test and evaluation of the Zarling and Burdick load cell models. CRREL Technical Note (unpublished).

Croasdale, K.R. (1974) The crushing strength of Arctic ice. *Proceedings, Symposium on Beaufort Sea Coastal and Shelf Resources.*

Danys, J.V. (1972) Effect of ice forces on some isolated structures in the St. Lawrence River. *Proceedings of 2nd International Symposium, International Association of Hydraulic Research, Leningrad.*

Dump, J.V. (1975) Effect of ice and wave forces on the design of Canadian offshore lighthouses. *Canadian Journal of Civil Engineering*, vol. 2, no. 2, p. 138-153.

Engelbrektson, A. (1977) Dynamic ice loads on a lighthouse structure. *Proceedings, Port and Ocean Engineering under Arctic Conditions Conference*, St. Johns, Newfoundland, Canada.

Korzhavin, K.N. (1971) Action of ice on engineering structures. U.S.S.R. Academy of Sciences, Siberian Branch. CRREL Draft Translation 260. AD723169.

Michel, B. (1970) Ice pressures on engineering structures. CRREL Cold Regions Science and Engineering Monograph III-B1b. AD709625.

Neill, C.R. (1976) Dynamic ice forces on piers and piles. An assessment of design guidelines in the light of recent research. *Canadian Journal of Civil Engineering*, vol. 3, no. 2, p. 305-341.

Peyton, H.R. (1966) Sea ice strength. University of Alaska Geophysical Institute Report 182.

Reinius, E., S. Haggord and L. Ernstsons (1971) Experience of offshore lighthouses in Sweden. *Proceedings, 1st Conference on Port and Ocean Engineering under Arctic Conditions*, Trondheim, Norway.

Sanden, E.J. and C. Neill (1968) Determination of actual forces on bridge piers due to moving ice. *Proceedings, Canadian Good Roads Association Conference (now Road Transportation Association, Canada)*, Toronto, Canada.

Schwarz, J. (1970) The pressure of floating ice-fields on piles. *Proceedings of 1st International Symposium, International Association for Hydraulic Research, Reykjavik, Iceland.*

Tryde, P. (1977) Intermittent ice forces acting on inclined wedges. CRREL Report 77-26. ADA046590.

APPENDIX A: FINDING LOAD MAGNITUDE AND LOCATION WITH A SINGLE REACTION BEAM DEVICE

The SRB cells installed on the Yukon River Bridge have the following linear geometry (see Fig. 11):

L_n = 36 in. L_r = 26 in. L_d = 18 in.

L_s = 13.5 in. L_{nr} = 5 in. L_{rd} = 4 in.

L_{ds} = 2.25 in.

Equation 12 states

$$P = \frac{(M_1 + M_2)}{L_{rd}} \tag{12}$$

so that if M_1 is 1000 in.-lbf and M_2 is 500 in.-lbf

$$P = \frac{1000+500}{4} = 375 \text{ lbf.}$$

Equation 16 states

$$X = \frac{L_n M_2}{M_1 + M_2} \text{ in.} \tag{16}$$

so that substitution of the above values for the SRB cell into eq 16 yields

$$X = \frac{36(500)}{1000+500} = 12 \text{ in.}$$

Thus, from the two moments, the geometry of the SRB cell and the above relationships, we find that the equivalent point load is 375 lbf at a point 12 in. from the left end of the nose piece.

Strain, not moments, will be measured in field use and eq 12, 16 and 19 can be modified to

$$P = \frac{C(\epsilon_1 + \epsilon_2)}{L_{rd}} \tag{A1}$$

and

$$X = \frac{L_n \epsilon_2}{\epsilon_1 + \epsilon_2} . \tag{A2}$$

These relationships are general and can be used for any single reaction beam device with equal or unequal loads symmetrically located on the beam.

APPENDIX B: FINDING LOAD MAGNITUDE AND LOCATION ON A DOUBLE REACTION BEAM DEVICE

The first device built was 18 in. square and is shown schematically in Figure 15. Two reaction beams are installed 11 in. apart and 3.5 in. from the sides of the device. The geometry of each individual reaction beam (the two have identical geometry) is as follows:

L_n = 18 in. L_r = 14 in. L_d = 10 in.

L_s = 7 in. L_{ni} = 2 in. L_{rd} = 2 in.

L_{ds} = 1.5 in. Y_1 = 3.5 in. Y_2 = 14.5 in.

By extension of eq 12 and 19

$$P = \frac{M_{1,1}+M_{1,2}+M_{2,1}+M_{2,2}}{L_{rd}}$$

$$= C\frac{(\epsilon_{1,1}+\epsilon_{1,2}+\epsilon_{2,1}+\epsilon_{2,2})}{L_{rd}} \qquad \text{(B1)}$$

where $M_{1,1}$, $M_{1,2}$, $\epsilon_{1,1}$ and $\epsilon_{1,2}$ are the moments and strains in beam 1 and $M_{2,1}$, $M_{2,2}$, $\epsilon_{2,1}$ and $\epsilon_{2,2}$ are moments and strains in beam 2 as shown in Figure B1. If the four moments are 40, 50, 60 and 100 in.-lbf respectively, P = 125 lbf.

If we wish to find the location of the load, we define a Cartesian coordinate system as shown in Figure B1 and treat each beam separately. The load on each reaction beam can be found using eq 12:

$$P_1 = \frac{M_{1,1}+M_{1,2}}{L_{rd}} = \frac{40+50}{2} = 45 \text{ lbf},$$

$$P_2 = \frac{M_{2,1}+M_{2,2}}{L_{rd}} = \frac{60+100}{2} = 80 \text{ lbf}.$$

The X value for the load on each beam can be found using eq A2. X_1 and X_2 are 10.0 and 11.25 in. respectively. X and Y for the equivalent point load can be found using the two equations

$$X = \frac{X_1P_1 + X_2P_2}{P_1+P_2} \qquad \text{(B2)}$$

$$Y = \frac{Y_1P_1 + Y_2P_2}{P_1+P_2} \qquad \text{(B3)}$$

By substituting the proper values and solving, X = 10.8 in. and Y = 8.62 in. This is the location of the equivalent point load.

It was pointed out earlier that the double reaction beam load cell has not been completely tested and evaluated. Consequently, some problems may develop which have not been identified.

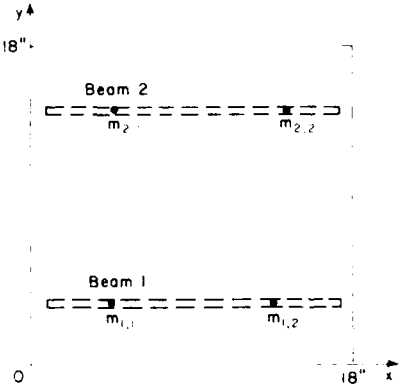

Figure B1. Coordinate system of a double reaction device.

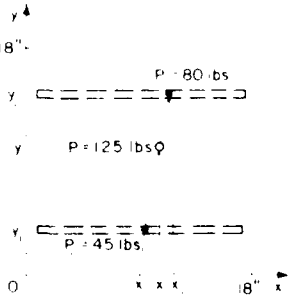

Figure B2. Solving for the location of P.

A fasimile catalog card in Library of Congress MARC format is reproduced below.

Johnson, P.R.
Single and double reaction beam load cells for measuring ice forces / by P.R. Johnson and J.P. Zarling. Hanover, N.H.: U.S. Cold Regions Research and Engineering Laboratory; Springfield, Va.: available from National Technical Information Service, 1980.
iii, 17 p., illus.; 28 cm. (CRREL Report 80-25.)
Prepared for Federal Highway Administration by Corps of Engineers, U.S. Army Cold Regions Research and Engineering Laboratory.
Bibliography: p. 14.
1. Ice forces. 2. Ice loads. 3. Instruments. 4. Load cells. 5. River ice. I. United States. Army. Corps of Engineers. II. Army Cold Regions Research and Engineering Laboratory, Hanover, N.H. III. Series: CRREL Report 80-25.

U.S. GOVERNMENT PRINTING OFFICE 1980- 700-417 249

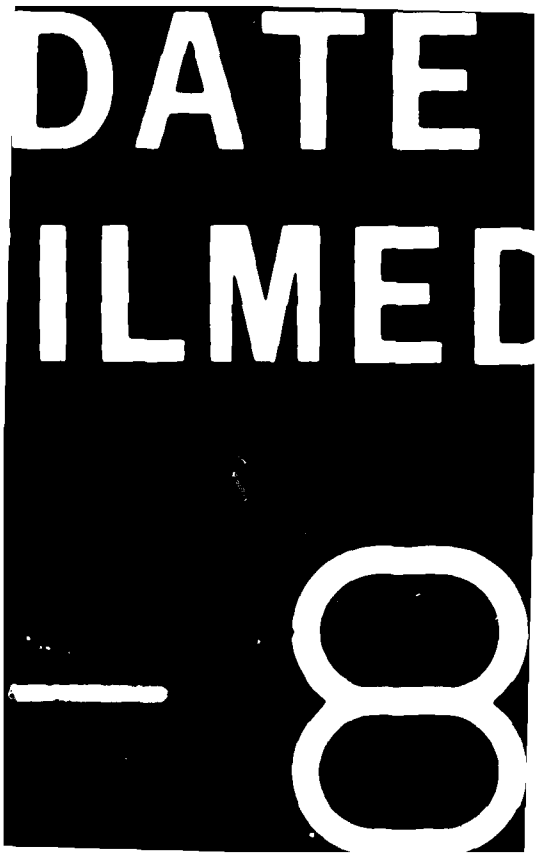
DATE
ILMED
8